Article

Human mesenchymal stem cells secrete hyaluronan-coated extracellular vesicles

Uma Thanigai Arasu[a], Riikka Kärnä[a], Kai Härkönen[a], Sanna Oikari[a], Arto Koistinen[b], Heikki Kröger[c,d], Chengjuan Qu[e], Mikko J. Lammi[e,f] and Kirsi Rilla[a]

a - Institute of Biomedicine, *University of Eastern Finland, Kuopio, Finland*
b - SIB Labs, *University of Eastern Finland, Kuopio, Finland*
c - Department of Orthopaedics and Traumatology, *Kuopio University Hospital, Kuopio, Finland*
d - Bone and Cartilage Research Unit, *Surgery, Institute of Clinical Medicine, University of Eastern Finland*
e - Department of Integrative Medical Biology, *Umeå University, Sweden*
f - School of Public Health, *Health Science Center of Xi'an Jiaotong University, Key Laboratory of Trace Elements and Endemic Diseases, National Health and Family Planning Commission, Xi'an, PR China*

Correspondence to Kirsi Rilla: *kirsi.rilla@uef.fi.*
http://dx.doi.org/10.1016/j.matbio.2017.05.001

Abstract

Extracellular vesicles (EVs) secreted by stem cells are potential factors mediating tissue regeneration. They travel from bone marrow stem cells into damaged tissues, suggesting that they can repair tissue injuries without directly replacing parenchymal cells. We have discovered that hyaluronan (HA) synthesis is associated with the shedding of HA-coated EVs. The aim of this study was to test whether bone marrow-derived hMSCs secrete HA-coated EVs. The EVs secreted by MSCs were isolated by differential centrifugation and characterized by nanoparticle tracking analysis. Their morphology and budding mechanisms were inspected by confocal microscopy and correlative light and electron microscopy. Hyaluronan synthesis of hMSCs was induced by lipopolysaccharide and inhibited by RNA interference and 4-methylumbelliferone. It was found that the MSCs have extremely long apical and lateral HA-coated filopodia, typical for cells with an active HA secretion. Additionally, they secreted HA-coated EVs carrying mRNAs for CD44 and all HAS isoforms. The results show that stem cells have a strong intrinsic potential for HA synthesis and EV secretion, and the amount of HA carried on EVs reflects the HA content of the original cells. These results show that the secretion of HA-coated EVs by hMSCs is a general process, that may contribute to many of the mechanisms of HA-mediated tissue regeneration. Additionally, an HA coat on EVs may regulate their interactions with target cells and participate in extracellular matrix remodeling.

Introduction

In the past couple of decades, therapeutic medicine options of stem cells have gained popularity because of the complications associated with regenerative treatments in the long terms [1–3]. The isolation of bone-forming progenitor cells from rat bone marrow stated that they resided in the stromal compartment of the bone marrow, which was the first step in identification of the human mesenchymal stem cells (hMSCs) [4]. Human mesenchymal stem (or stromal) cells are multipotent adult stem cells that can differentiate into muscle cells, chondrocytes, osteoblasts and adipocytes. Because of their ex vivo expansion capacity and fewer ethical concerns, the MSCs are gaining increasing credibility as therapeutic agents [5]. Their broad distribution throughout the body makes them a critical factor in various research and clinical trials as regenerative agents for diseases such as cancer, Alzheimer's disease, osteoarthritis, liver cirrhosis, and myocardial infarction [6].

Though there have been tremendous advances in research using stem cells, extracellular vesicles (EVs) originating from stem cells may have equal therapeutic

benefits [1]. The EVs are plasma membrane-derived particles, ranging from 30 nm to 1000 nm in diameter, and they are secreted into the extracellular environment, which acts as a communication channel. They are able to carry and transfer compounds, such as proteins, RNA, and even DNA, from their cells of origin to other cells during embryonic development, wound healing and other tissue injuries, inflammation, and cancer [7]. Almost all cell types secrete EVs into the extracellular environment [8,9], including stem cells [10]. The EVs secreted by stem cells have been shown to be essential factors for tissue healing and regeneration [11]. They can also transfer information between bone marrow MSCs and damaged tissue in acute injuries [12], suggesting that MSCs can repair damaged tissues without directly replacing parenchymal cells.

Hyaluronan (HA) is a unique glycosaminoglycan synthesized at the inner leaf of the plasma membrane by three isoenzymes, hyaluronan synthases (HAS)1–3 [13]. HA is crucial for the assembly of growth-promoting pericellular matrices and has a significant contribution to cell proliferation, migration, differentiation and embryogenesis, as well as to the progression of malignant tumors [14]. Because of these characteristics, it is also considered an essential component of the stem cell niche [15] and a suppressor of immune responses [16]. However, its role in the regulation of stem cell differentiation is a complicated and inadequately defined process. Interestingly, one of the commonly used specific markers for stem cells is CD44, a receptor that interacts with HA [17,18]. In recent years, many articles have indicated the potential of HA in stem cells [19,20], and it is known that stem cells express high levels of all three HAS enzymes [21]. We have previously shown that the active HAS isoenzymes (HAS2–3) in the plasma membrane are responsible for the growth of long membrane protrusions, thereby altering the overall shape of the plasma membrane [22]. We were also able to observe shedding of the EVs from these long protrusions that were positive for EGFP-tagged HAS3 [23] and showed that the overexpression of GFP-HAS3 stimulates the shedding of the EVs that carry HA on their surface.

As discussed above, the MSCs secrete EVs and produce high levels of HA, suggesting that MSC-derived EVs could carry HA on their surface. To confirm this hypothesis we characterized the EVs secreted by the bone marrow-derived hMSCs and their relationship with HA and its synthesis. We found that HA is carried on the plasma membrane of the EVs that originate from filopodia and retraction fibers, and the amount of HA carried on EVs corresponds to the HA synthesis activity of the original cells. The HA-coated EVs secreted by the hMSCs are potential therapeutic and diagnostic tools and targets of therapy.

Materials and methods

Cell culture

Human bone marrow material samples were collected from surgical specimens at the local university hospital during hip joint replacement operations (North-Savo Health Care District Ethical Committee license no. 62//2010). Human bone-marrow-derived MSCs were isolated and characterized as previously described [21]. The cells were cultured in MEM alpha (HyClone, ThermoFisher Scientific, Erembodegem, Belgia) supplemented with 10% FBS (HyClone), 10 ng/ml basic fibroblast growth factor (bFGF, PeproTech, New Jersey, USA), 25 µg/ml vitamin C (Sigma Aldrich, Missouri, USA), 50 µg/ml streptomycin sulphate, and 25 U/ml penicillin (EuroClone). Cells with passage numbers 1–4 were used for experiments. For experiments with the EV isolation, FBS was purified [24] by centrifugation at 100000 ×g for 16 h and sterile-filtered with 0.2 µm filters (Minsart, Sartorius Stedim, Biotech, Goettingen, Germany). Various concentrations of lipopolysaccharide (LPS, Sigma) and 4-methylumbelliferone (4-MU, Sigma) were used in the present study.

Vital stainings

For staining of the pericellular HA coat of live cells, a fluorescently labeled (Alexa Fluor 594) HA binding complex (fHABC) was used as described previously [25]. Live cell cultures grown on chambered coverglasses (Ibidi GmbH, Martinsried, Germany) were incubated for 2 h at 37 °C with 2 µg/ml of fluorescent HABC in culture medium. CellMask™ Deep Red plasma membrane stain (1.25 µg/ml, Molecular Probes, Eugene, OR) was added to the cultures immediately before imaging to label the plasma membranes.

Immunostaining of CD44 and staining of HA in fixed cells

The cells were cultured on chambered coverglasses (Ibidi) as monolayers or to trap a higher number of the EVs under a 3D basement membrane extract gel, Cultrex® (Trevigen Inc., Gaithersburg, MD). For fluorescent stainings, the cells were fixed with 4% paraformaldehyde in phosphate-buffered saline (PBS), pH 7.4, for 1 h. The gels were incubated in glycine (200 mM) in PBS for 20 min to quench the excess aldehyde. The samples were washed with PBS, permeabilized for 20 min at room temperature with 0.1% Triton-X-100 in 1% BSA, and incubated overnight at 4 °C with anti-CD44 monoclonal antibody (Hermes 3, 1:100, a generous gift from Dr. Sirpa Jalkanen, University of Turku, Finland). After washing, the cells were incubated overnight with fluorescently

Table 1. Quantitative real-time RT-PCR primer sequences.

Gene		Primer sequences	
Hyaluronan synthase 1	**HAS1**	Forward 5′	CAAGATTCTTCAGTCTGGAC
		Reverse 5′	TAAGAACGAGGAGAAAGCAG
Hyaluronan synthase 2	**HAS2**	Forward 5′	CAGAATCCAAACAGACAGTTC
		Reverse 5′	TAAGGTGTTGTGTGTGACTG
Hyaluronan synthase 3	**HAS3**	Forward 5′	CTTAAGGGTTGCTTGCTTGC
		Reverse 5′	GTTCGTGGGAGATGAAGGAA
CD44	**CD44**	Forward 5′	CATCTACCCCAGCAACCCTA
		Reverse 5′	CTGTCTGTGCTGTCGGTGAT
Ribosomal protein, Large, P0	**Rplp0**	Forward 5′	AGATGCAGCAGATCCGCAT
		Reverse 5′	GTGGTGATACCTAAAGCCTG

labeled secondary antibodies (Vector Laboratories Inc., Burlingame, CA, I:1000). For HA staining, monolayer cultures were incubated overnight at 4 °C with 3 µg/ml of biotinylated HA-binding complex (bHABC). After washing, the sections were incubated for 1 h with Texas red-labeled streptavidin (Vector, 1:200). Nuclei were labeled with 4′,6-diamidino-2-phenylindole (DAPI, 1 µg/ml, Sigma).

Confocal microscopy

The fluorescent images were obtained with a Zeiss Axio Observer inverted microscope (40 × NA 1.3 oil or 63 × NA 1.4 oil –objectives) equipped with a Zeiss LSM 700 or LSM800 confocal module (Carl Zeiss Microimaging GmbH, Jena, Germany). For live cell imaging, Zeiss XL-LSM S1 incubator with temperature and CO_2 control was utilized. The ZEN 2012 software (Carl Zeiss Microimaging GmbH) was used for image processing and 3D rendering.

Transmission electron microscopy (TEM)

The EV preparations were layered onto carbon-coated glow-discharged copper grids. Grids were fixed in 2% paraformaldehyde for 10 min and contrasted using 2% neutral uranyl acetate for 10–15 min and embedded in 1.8% methyl cellulose (25 Ctp)/ 0.4% uranyl acetate. Imaging was performed with a JEOL JEM 2100F transmission electron microscope (Jeol Ltd., Tokyo, Japan) operated at 200 kV.

Correlative light and electron microscopy

Cells were grown on gridded glass bottom culture dishes (MatTek Corporation, Ashland, MA) for re-localization of cells during imaging. Correlative light and electron microscopy (CLEM) was performed as previously described [26]. The cells were fixed with 2% (v/v) glutaraldehyde, fluorescently stained as described above, and imaged with the Zeiss LSM 700 confocal module and an external DIC-capable transmitted-light channel. After processing for scanning electron microscopy, including dehydration and coating with gold, the cells were imaged with Zeiss Sigma HD|VP (Zeiss, Oberkochen, Germany) at 3 kV.

Hyaluronan ELSA

Subconfluent cell cultures on 24-well plates were used to measure the HA secretion. After treatment or transient transfections, fresh medium was provided (with 5% FBS), and cells were cultured for 24 h before the cells were counted and the media harvested for the sandwich type HA ELSA assay as described previously [27]. To measure the HA content of the EV fractions, cell debris was removed from culture media by centrifugation at 1000 × *g* for 5 min, the supernatants were centrifuged at 20000 × *g* for 90 min at 4 °C and the pellet was subjected to ELSA assay.

Nanoparticle tracking analysis (NTA)

The size distribution and number of the EVs in hMSC culture media were analyzed with the Nanoparticle Tracking Analyzer (Malvern Instruments Ltd., Malvern, UK) with an NS300 view unit. The conditioned culture media were centrifuged at 1000 × *g* for 5 min to remove cell debris. The supernatants were centrifuged at 11,000 × *g* or 2000 × *g* for 90 min at 4 °C and the pellet was suspended in PBS and diluted 1:20 in PBS before the analysis. The following settings were used for data acquisition: camera level 13, acquisition time 30 s and detection threshold 3. Data analysis was performed with the NTA 3.1 software (NanoSight, Amesbury, UK). Data for each sample were obtained from four replicates.

RNA interference

The HAS and scrambled siRNAs were obtained from Ambion (ThermoFisher Scientific Waltham, MA, USA). Cells were grown on six-well plates until 50% confluence, and treated with 30 nM siRNA using Lipofectamine RNAiMax reagent (Invitrogen) according to the manufacturer's instructions. The cells were grown for 48 h before analysis.

Quantitative real-time RT-PCR (qRT-PCR)

For RNA isolation from the EVs, conditioned media were first filtered through a 5 μm filter (Sartorius, Goettingen, Germany) to remove floating cells, followed by centrifugation at 1000 × *g* for 10 min. The supernatant was centrifuged at 100,000 × *g* for 90 min to pellet the EVs. Total RNA from the cells and the EV fractions were isolated using Tri Reagent (Molecular Research Center Inc., Cincinnati, OH, USA). The cDNAs were synthesized using the Verso cDNA kit (Thermo Scientific). The quantitative real-time PCR was performed with Fast Start Universal SYBR Green mix (Roche Applied Science, Indianapolis, IN, USA) using the Stratagene Mx3000P real-time PCR system (Agilent Technologies, Santa Clara, CA, USA). Relative mRNA expression levels were compared by using the 2 − ΔΔC(T) method, with ribosomal protein, large, P0 (Rplp0) as the reference gene. The primer sequences are given in Table 1.

Statistical methods

Statistical analyses were carried out using the GraphPad Prism version 5.00 for Windows, (GraphPad Software, San Diego, CA, USA) or IBM SPSS Statistics 22 for Windows (IBM Corporation, Armonk, NY, USA). The significance of differences between groups was tested using one-way analysis of variance (ANOVA) with post hoc tests or the one-sample *t*-test. Differences were considered significant when $p < 0.05$.

Results

Human MSCs have hyaluronan-coated filopodia that act as vehicles for EVs carrying a thick hyaluronan coat

Confocal 3D imaging of the live hMSCs labeled with fHABC showed a thick HA coat surrounding the plasma membrane and its long protrusions (Fig. 1A). Additionally, a high number of HA-coated EVs attached to the bottom of the plate were detected (arrows, Fig. 1A). The relative HA content of the conditioned culture medium, the supernatant after the final ultracentrifugation step representing "free HA" and the pelleted EV fraction were quantified with HA assay. The results showed that a main proportion of secreted HA (382 ng/10,000 cells/24 h) is in a free form in the culture medium, but the EV fraction contains a notable concentration (11 ng/10,000 cells/24 h) of HA (Fig. 1B).

Additionally, the mRNA expression levels of the HA-associated proteins (CD44 and HAS isoforms) in the hMSCs and the EV fractions were quantified with qRT-PCR. All three HAS isoforms, as well as CD44, were expressed by the cells and carried by the EVs (Fig. 1C). The results show also that the relative mRNA expression levels of HASs and CD44 carried by the EVs reflected those of the original cells (Fig. 1C).

To confirm that the HA-positive EVs were derived from the plasma membrane, double staining with a plasma membrane marker and fHABC was used. The staining showed in more detail the numerous long plasma membrane protrusions, surrounded by a thick HA coat (Fig. 1D–F). The "hedgehog"-like morphology of the cell is demonstrated in vertical views (Fig. 1D–F). Additionally, plenty of plasma membrane-derived HA-positive EVs that adhered to the bottom of the plate were detected around the cells (white box in Fig. 1F). A higher magnification of this area (Fig. 1G) shows that the plasma membrane-derived EVs (arrows in Fig. 1G), which had diameters ranging from <100 nm to 1 μm, were coated with a thick HA layer (Fig. 1H–I). Supplementary movies 1 and 2 show the shedding of the fHABC-positive EVs in the live hMSCs and the formation of HA positive "fingerprints" as a result of the retraction of plasma membrane protrusions (arrows in Supplementary movie 2).

The EVs of variable diameter secreted by hMSCs are positive for CD44

To further characterize the EVs secreted by the hMSCs, the cells were fixed and immunostained with CD44 antibody. The vertical view showed protrusions that were shorter and lower in number (Fig. 2A–B) compared to those of the plasma membrane-labeled live cells (Fig. 1A). As previously reported [22,25], the plasma membrane protrusions easily shrink and collapse during fixation. Shedding of the CD44-positive EVs of variable size was seen near the plasma membrane (arrows in Fig. 2A). Some large EVs or blebs on the plasma membrane were also detected (arrow-heads in Fig. 2A). Imaging with SEM showed the collapsed filopodia and the EVs on the apical surface of the cells (Fig. 2C). The EVs isolated from the culture medium with ultracentrifugation were analyzed by TEM (Fig. 2D), and the size distribution of the preparations were analyzed by NTA (Fig. 2E). The results showed that the main population of the EVs in the culture medium was between 100 and 200 nm in diameter. The diameter of 96.5% of the measured particles was below 300 nm, while 3.5% of the particles were between 300 and 1000 nm.

Correlative light and electron microscopy shows the morphology of CD44 and HA-positive EVs secreted by the hMSCs

Correlative light and electron microscopy was utilized to analyze the morphology of HA and CD44 carried by the EVs. Fixation partly destroyed and aggregated the cell-associated HA coat, but high levels of HA (Fig. 3A) and CD44 (Fig. 3B) were detected on the plasma membrane and its protrusions. Hyaluronan

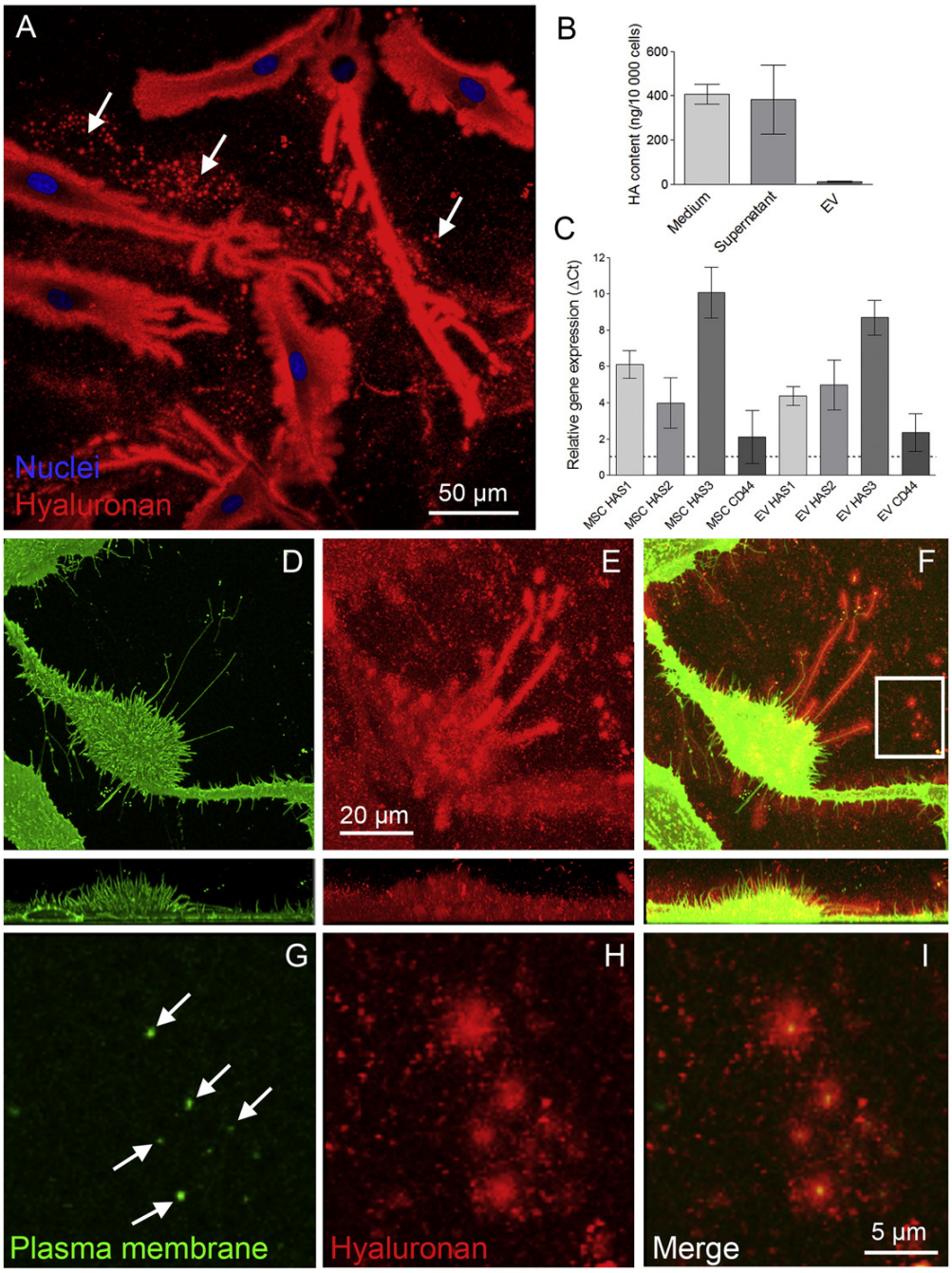

Fig. 1. *Human MSCs display long hyaluronan (HA)-coated filopodia and secrete plasma membrane-derived vesicles surrounded by a thick HA coat.* Horizontal 3D projection created from confocal optical sections of the live hMSCs labeled with HA-binding probe (red). Arrows point to the HA-positive EVs (A). The HA content of the conditioned culture medium, the EV fraction, and the remaining supernatant after ultracentrifugation, the mean ± S.E. of 3 independent experiments is shown (B). The mRNA expression levels of the most important proteins related to HA metabolism in the hMSC cells and in the EVs secreted by them, presented as ΔCt values and the mean ± S.E. of 4–5 experiments are shown (C). 3D projections of one cell double-labeled with plasma membrane marker (D and G, green) and HA-binding probe (E and H, red). Merged images are shown in F and I. Vertical views presented below each panel (D–F) demonstrate the hedgehog-like morphology typical off cells producing high amounts of HA. Panels G–I show the area indicated by a white box in panel F with higher magnification, showing HA-coated plasma membrane-derived EVs adhered to the bottom of the dish (arrows in G).

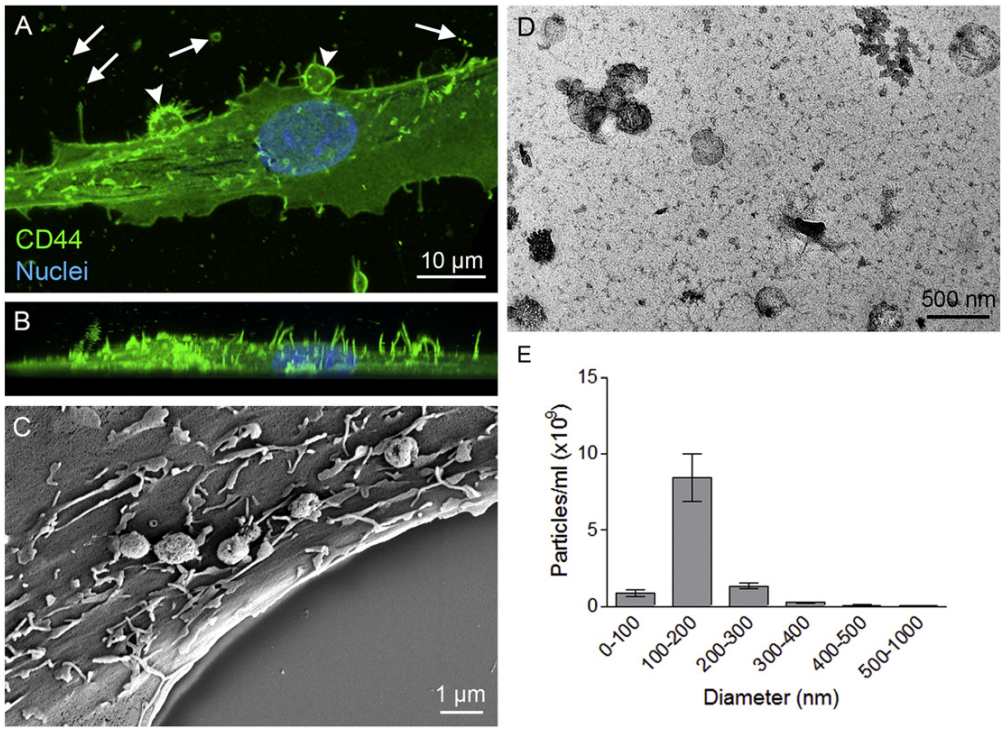

Fig. 2. *Characterization of the EVs secreted by the hMSCs indicate that the hMSCs secrete EVs of variable size*. A high magnification 3D confocal horizontal (A) and vertical (B) view of a fixed and CD44-immunostained hMSC. Panel (C) shows a SEM image of the EVs budding from the cell surface, and (D) shows a TEM image of negative staining of the EVs isolated from the culture medium of the hMSCs. Panel (E) demonstrates the size distribution of the EVs secreted by the hMSCs, analyzed by NTA. Means ± S.E. of 4 independent experiments are shown.

and CD44 were also partially colocalized (Fig. 3C). Arrows in the confocal (Fig. 3D) and corresponding SEM image (Fig. 3E) point to the CD44- and HA-positive EVs of variable size attached to the bottom of the plate.

A high-resolution SEM image of one of the EVs (indicated by a red arrow in Fig. 3D and E) shows the rough surface morphology of the vesicle (Fig. 3F). In addition to the blebbing from the plasma membrane or its protrusions, CLEM imaging revealed CD44 and HA-positive EVs (Fig. 4), forming "footprints" that originate from retraction fibers (Fig. 4A–C). Additionally, the EVs formed as a result of vesiculation of thin CD44 and HA positive plasma membrane protrusions were detected (Fig. 4D–I).

Lipopolysaccharide induces filopodial growth, plasma membrane blebbing, HA secretion, and HAS expression in the hMSCs

To investigate the effect of LPS on the HA secretion in the hMSCs, the cells were treated with different concentrations of LPS. First, the effect of LPS on the cellular morphology and EV secretion was studied by confocal microscopy in CD44 immunostained 3D cultures. Because in monolayer cultures the EVs tend to shed quickly into the culture medium after detachment from the plasma membrane (Supplementary movies 3 and 4), the cells were grown under basement membrane extract gel to trap higher numbers of EVs for detection. Compared to control cells (Fig. 5A, C), the LPS-treated cells obtained a more spindle-shaped morphology (Fig. 5B, D). Additionally, a higher number of CD44-positive protrusions were detected, especially on the apical faces of the cells (Fig. 5D). A higher magnification of the LPS-treated cells showed EVs of variable size budding from the plasma membrane, especially from protrusions and their tips (arrows in Fig. 5E). The cell-associated HA staining around the live LPS-treated hMSCs and their protrusions (Fig. 5G) was increased compared to the untreated cells (Fig. 5F).

The effect of LPS on the activity of HA secretion was analyzed by measuring HA concentrations in the culture media of the cells (Fig. 5H). Hyaluronan secretion was increased with all used concentrations of LPS (1.4–1.7-fold) and reached a statistical significance ($p < 0.05$) at 50–150 ng/ml. To quantify the effect of LPS on the EV secretion, the concentrations of particles secreted into the culture media of

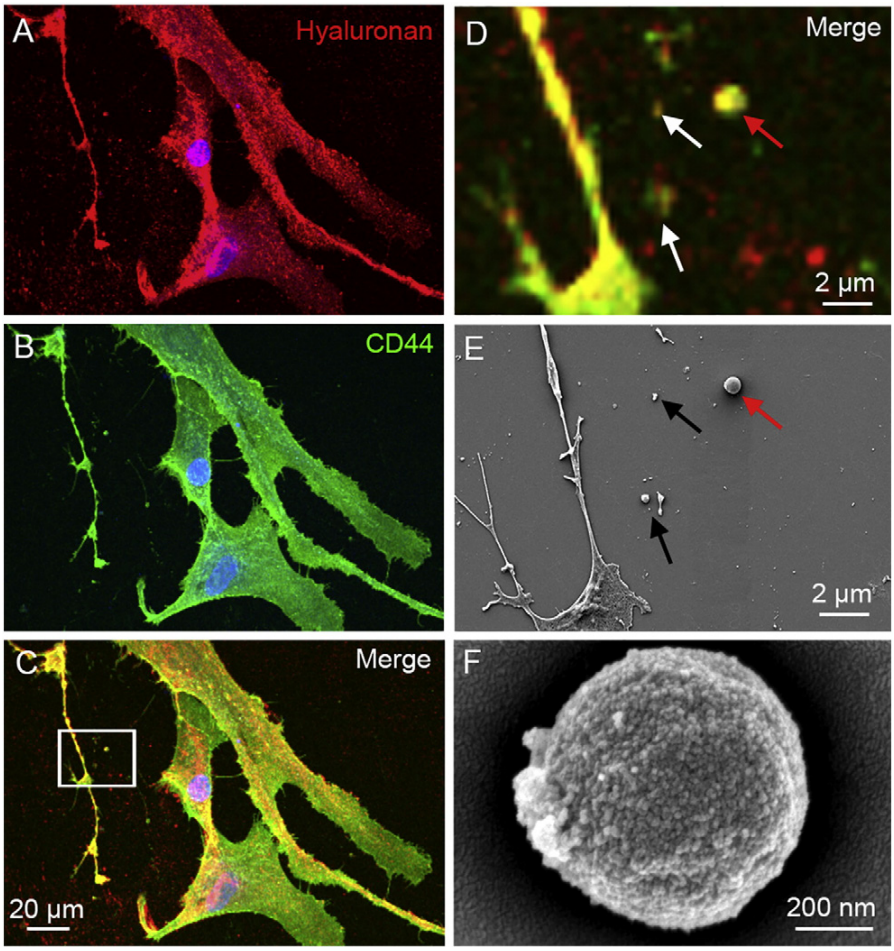

Fig. 3. *Analysis with CLEM shows that the EVs shed by the hMSCs carry HA and CD44 and have a rough surface morphology*. (A) HA staining, (B) CD44 immunostaining, and (C) merged confocal image of the fixed hMSCs. (D) A higher magnification image of the area indicated by a white box in C, (E) SEM image of the same area, and (F) a high-resolution SEM image showing the surface ultrastructure of a single EV (indicated by red arrow in D and E). Arrows in D and E point to the EVs of different size that adhered to the bottom of the dish. All confocal images are horizontal views created from stacks of optical sections.

monolayer cultures were measured by NTA. No significant differences in the total number of particles were detected (Fig. 5I). However, the HA content of the EV fractions was increased with relatively similar levels as in culture media upon LPS-treatment (Fig. 5J), which suggests that the HA content of EVs reflects the HA synthesis activity of parent cells. The LPS treatment induced significant increases in the mRNA expression levels of all HAS isoforms with all LPS concentrations (Fig. 5K–M).

Inhibition of HAS expression does not significantly decrease the HA secretion of the MSCs

The inhibition of mRNA expression of HAS2 and HAS3 by RNA interference was applied to observe the effect of HAS inhibition on the hMSC HA secretion, morphology, and the EV production. Inhibition of HAS2 resulted in a statistically significant downregulation of HAS2 expression levels (74%, Fig. 6A). Simultaneous inhibition of HAS2 and HAS3 resulted in a lower level of decrease in HAS2 expression (45%). Inhibition of HAS3 resulted in a significant decrease in HAS3 expression (62%, Fig. 6B). Simultaneous inhibition of HAS2 and HAS3 resulted in similar level of inhibition on the HAS3 mRNA expression levels (55%) as HAS2 siRNA alone (Fig. 6B), similarly to the HAS2 mRNA expression (Fig. 6A).

ELSA assays showed that HAS2 inhibition resulted in a 47% decrease in HA secretion (Fig. 6C). However, HAS3 inhibition did not affect the total HA secretion (Fig. 6C). Simultaneous inhibition of HAS2 and HAS3

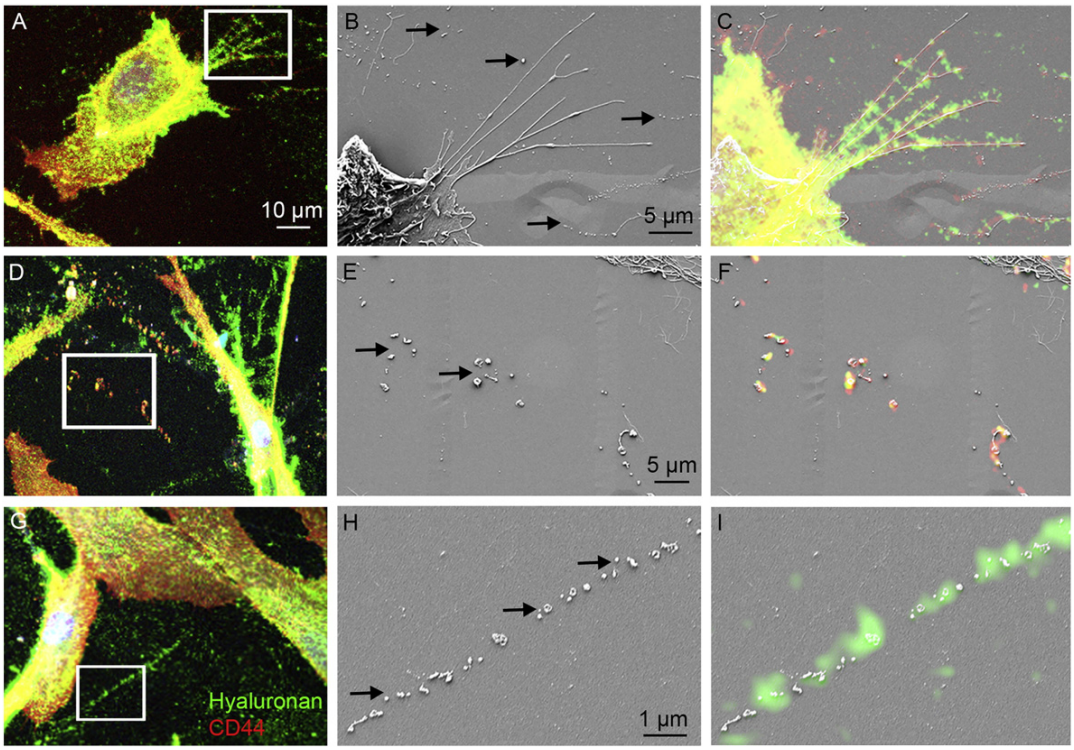

Fig. 4. *Multiple mechanisms for shedding of CD44- and HA-positive EVs*. Correlative light and electron microscopy of the hMSC stained for CD44 and HA, showing the EVs that originate from the tips of protrusions (A–C) or vesiculation of long projections or retraction fibers (D–I). Maximum intensity projections are shown in A, D, and G, SEM images from the areas indicated by white boxes in B, E, and H and overlay images of SEM and fluorescent signal in C, F, and I. Arrows point to the EVs of different size.

downregulated HA secretion with a similar level (44%) as that of HAS2 inhibition alone (Fig. 6C). In confocal analysis, no visible differences in the number of CD44-positive filopodia or in the EVs upon HAS inhibition were detected (Fig. 6D–G). However, HAS2 inhibition resulted in decreased cell-associated HA, especially around filopodia (Fig. 6I) compared with control cells (Fig. 6H), and CLEM showed a decreased number of HA- and CD44-positive filopodia in HAS2 siRNA-treated monolayer cultures (Fig. 7). Particle counting with NTA showed no effects on the particle concentrations in the culture media upon HAS inhibition (Fig. 6J). The HA content of the secreted EVs (Fig. 6K) reflected the HA synthesis activity of the cells (Fig. 6C), but no significant decrease was detected.

4-MU downregulates HAS1 and HAS2 expression and HA secretion of the hMSCs

Treatment with 4-MU, a general inhibitor for HA synthesis, resulted in decreased (Fig. 8B) intensity of the cell-associated HA coat and HA-coated protrusions (arrows in Fig. 8A) and in a decreased number (Fig. 8D) of CD44-positive protrusions and the EVs (arrows in Fig. 8C) when grown under 3D gel. As measured from the culture media, HA secretion decreased by 23%, 36% ($p < 0.05$), and 35% ($p < 0.05$) with 0.2 mM, 0.5 mM, and 1 mM 4-MU, respectively (Fig. 8E). The relative HA content of the EV fraction decreased with a similar magnitude as in the culture media (Fig. 8F), indicating that the HA content of the EVs reflected the HA synthesis activity of original cells. The NTA analysis showed no significant effect by 4-MU in EV secretion into the culture medium (Fig. 8G). Treatment with 4-MU resulted in statistically significant (0.5 mM, $p < 0.01$; 1 mM, $p < 0.005$) decrease in HAS1 (Fig. 8H) and HAS2 (Fig. 8I) mRNA expression levels. Surprisingly, expression levels of HAS3 increased, but no statistical significance was found (Fig. 8J).

Discussion

Activity of HA synthesis, filopodia and budding of EVs are connected to each other

The results of the present study demonstrated that the MSCs derived from human bone marrow express

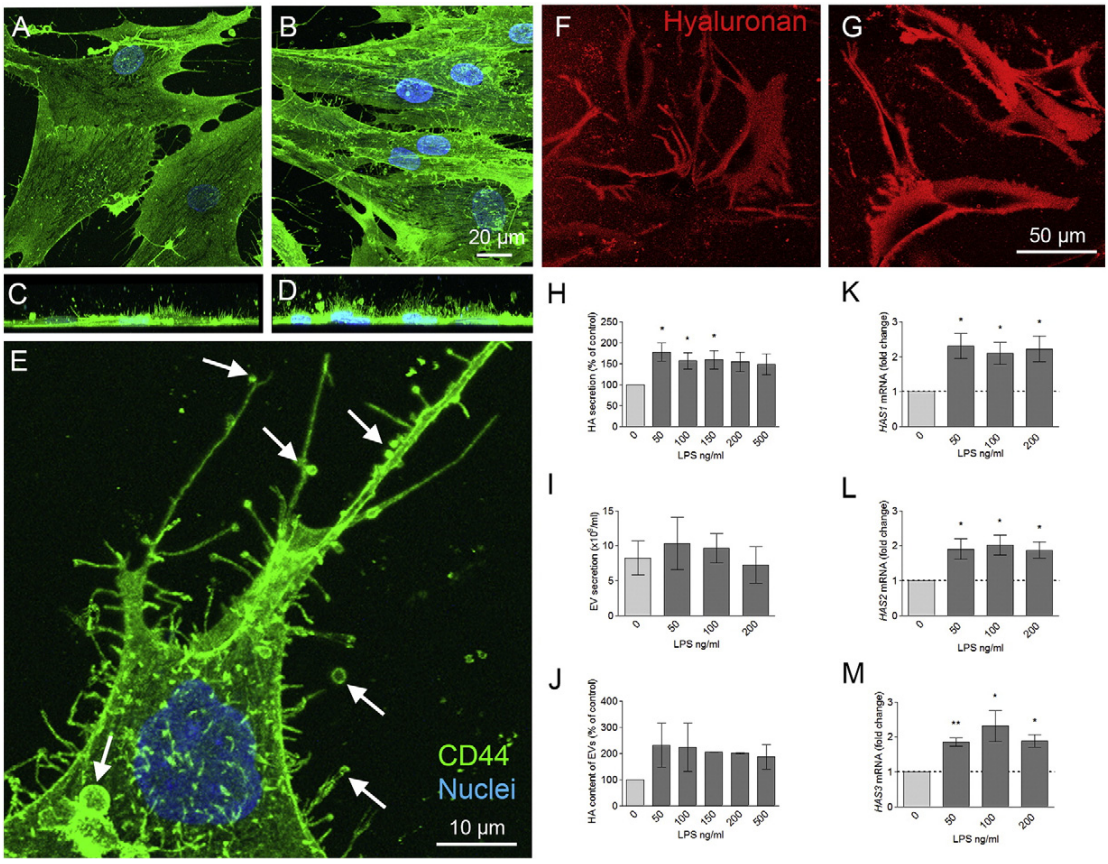

Fig. 5. *Lipopolysaccharide (LPS) treatment induces growth of CD44- and HA-positive filopodia and enhances HA secretion and expression levels of HAS isoforms in the hMSCs.* Horizontal (A and B) and vertical (C and D) views of control (A and C) and LPS (100 ng/ml) treated (B and D) hMSCs grown under basement membrane extract gel. A higher magnification image of a LPS-treated cell (E) showing the EVs budding from the plasma membrane and its protrusions (arrows). Panels A–E are projections created from stacks of confocal optical sections. The confocal optical sections of the live cells labeled with fHABC to detect the HA coat in control (F) and LPS-treated (100 ng/ml) cells (G). Hyaluronan secretion levels measured from the culture media (H), the EV concentrations in the culture media (I), and HA content in the EV fractions (J). Expression levels of HAS1 (K), HAS2 (L), and HAS3 (M) in the hMSCs treated with different concentrations of LPS. The means ± S.E. of six independent experiments are shown in H, the means ± S.E. of two experiments in I, and means ± S.E. of four to six experiments in J–M, $*p < 0.05$, $**p < 0.01$, compared with 0 ng/ml of LPS by a one-sample *t*-test.

HA-coated filopodia and secrete EVs that carry HA on their surface. The results support the theory that HA synthesis takes place on plasma membrane protrusions [22]. Additionally, we show in human primary cells that HA is carried on the surface of the EVs that originate from the tips of HA-synthesizing filopodia, as shown previously in immortalized cell lines [23,28]. Interestingly, live cell imaging and CLEM showed that EVs are assembled by diverse mechanisms, such as direct budding from the plain plasma membrane, shedding from the tips of protrusions, or vesiculation of long projections or retraction fibers. These diverse shedding mechanisms may be a reason for the variable size of EVs, which is in line with several recent findings [29–31].

The synthesis of HA along the long protrusions may be important especially in tissues with a low number of cells and high volume of ECM, such as loose connective tissues, bone, and cartilage. In these tissues, the diffusive transport of HA into a matrix distant from the cell body may be low. With the aid of long protrusions and shedding EVs, horizontal transfer, and the deposition of HA, other ECM components, and signaling molecules [2] can be distributed even at sites distant from the cell of its origin. Thus, future experiments are required to show the role of filopodia

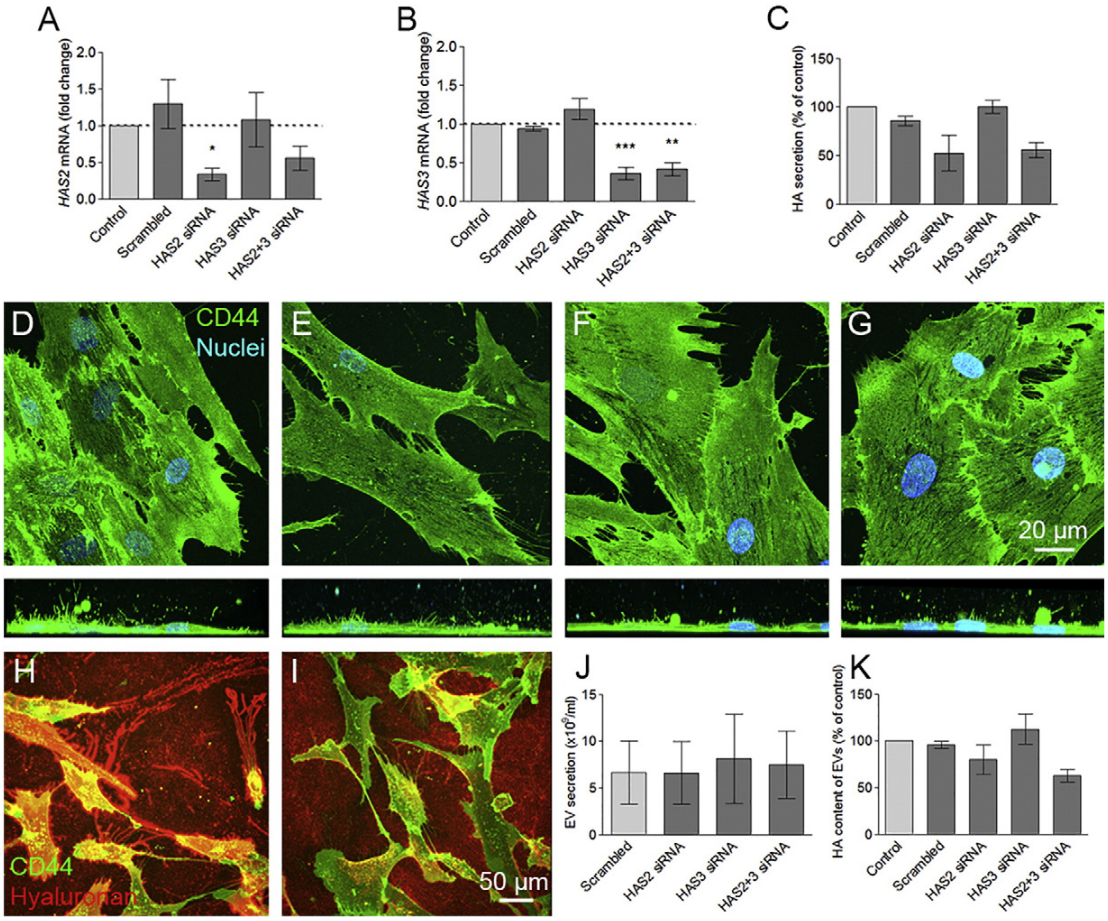

Fig. 6. *Effect of HAS2 and HAS3 RNA inhibition on the mRNA expression levels of HAS2 and HAS3, HA secretion, and the EV shedding of the hMSCs*. mRNA expression levels of *HAS2* (A), *HAS3* (B) and levels of HA secretion (C) upon RNA inhibition of *HAS2* and *HAS3*. Morphology visualized by CD44 immunostaining of scrambled siRNA (D), *HAS2* RNAi (E), *HAS3* RNAi (F), and *HAS2* and *HAS3* RNAi (G). Horizontal and corresponding vertical views are shown in each panel. Double staining with plasma membrane marker (green) and HA (red) of scrambled siRNA (H) and *HAS2* siRNA (I)–treated live cells. The EV concentrations in culture media (J) and HA contents of the EV fractions (K). Means ± S.E. of four to seven independent experiments are shown in A–B, two experiments in J, and three experiments in C and K. $*p < 0.05$, $**p < 0.01$, $***p < 0.001$, compared with the scrambled siRNA by ANOVA.

and HA-EVs as matrix depositors and their ability to create niches that preserve stemness.

Hyaluronan receptor CD44 is a potential marker for the EVs

This work shows that the HA receptor CD44 is a powerful marker for microscopic detection of the EVs, especially when they are trapped inside a 3D matrix. Fluorescent labeling of CD44 combined with SEM confirmed that vesicles even below the resolution limits of light microscopy can be detected with CD44 immunostaining. In previous studies, CD44 has been shown to be carried by the EVs secreted by the MSCs and to regulate EV interactions with target cells [29,32]. We have recently shown that primary mesothelial cells are induced to secrete CD44-positive EVs upon the induction of epithelial to mesenchymal transition (EMT) by EGF or wounding [33]. These observations suggest that CD44 is a potential marker for the EVs, especially those secreted from stem cells or activated cells in tissue injuries or other pathological conditions.

As previously shown, CD44 is a biomarker to identify MSCs [17,18] and cancer stem cells in many different types of tumors [34]. It is an important factor also in the generation of stem cell niche [35], and its interactions with HA are essential for the trafficking of MSCs and their homing on the bone marrow, where they are maintained in an undifferentiated state [15]. Additionally, an extensive HA coat assembled by

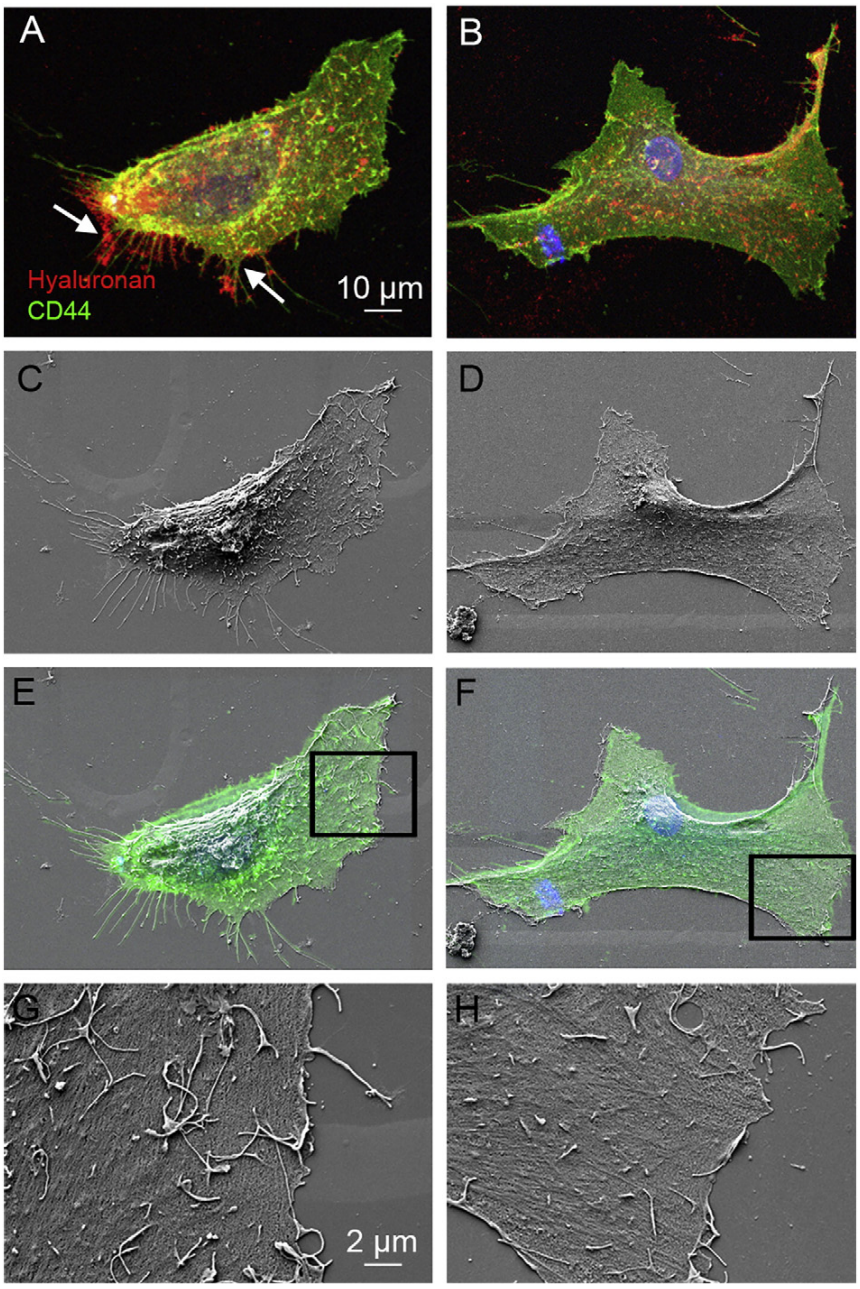

Fig. 7. *Effect of HAS2 inhibition on the HA-coated filopodia imaged by CLEM.* A control siRNA-treated cell is shown in A, C, E, and G and a HAS2 siRNA-treated cell in B, D, F, and H. Arrows in (A) show HA- and CD44-positive plasma membrane protrusions. Confocal 3D projections are shown in A and B, corresponding to SEM images in C and D, overlaid with CD44 signal and SEM images in E and F and higher magnification of the areas indicated by black boxes in G and H.

CD44 [21] may regulate the interactions between EVs, their target cells, and ECM [36]. In summary, both CD44 and HA, carried by the vesicles, may create regenerative scaffolds for growing and healing of the tissues, regulation of immune responses, and targeting of EVs to their recipient cells.

The hMSCs have a strong intrinsic potential for HA secretion

Consistent with previous observations [21], our present results show that the hMSCs themselves produce high levels of HA, which means that they

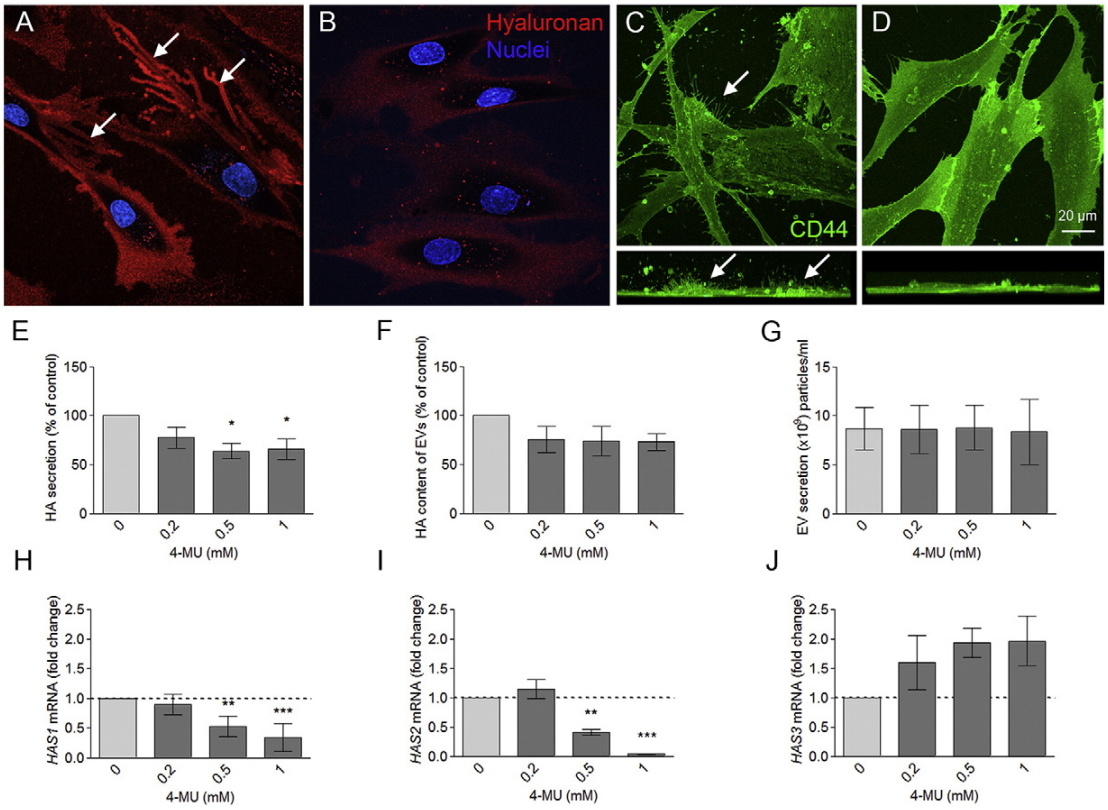

Fig. 8. *Effect of HA synthesis inhibitor on hMSC HA secretion and EV shedding.* Cell-associated HA labeled with fHABC (red) in the live control cells (A) and cells treated with 0.5 mM 4-MU (B). CD44 immunostaining of the fixed control (C) and 4-MU-treated (D) (0.5 mM) cultures. Horizontal and corresponding vertical views are shown in both panels. Effect of 4-MU on HA content of the culture media (E) and the isolated EV fractions (F). Arrows in A and C point to the HA- and CD44-positive filopodia. Panels G, H, I, and J show the effect of 4-MU on EV secretion and *HAS1*, *HAS2*, and *HAS3* mRNA expression, respectively. Means ± S.E. of four independent experiments are shown in E and F, and means ± S.E. of three to four experiments are shown in G–J, $*p < 0.05$, $**p < 0.01$, $***p < 0.001$, as analyzed by ANOVA.

participate in the creation of the HA-rich stem cell niche in an autocrine way. Interestingly, the inhibition of HAS2 and HAS3 expression by siRNA transfections or 4-MU treatment resulted in maximally only a 47% and 35% decrease in the total HA secretion, respectively. Post-transcriptional regulation of HASs [37] is a potential explanation for the weak effect of inhibitors on HA secretion levels.

LPS was utilized to stimulate the HA synthesis of stem cells in the present study. It is known to induce inflammatory reaction in many cell types [38,39], increase HAS expression and HA secretion [40], and induce the EV shedding [41] of macrophages. Our present results show that LPS induce HA synthesis, HAS expression, and CD44-positive filopodia formation of hMSCs. Interestingly, it is also possible that presenting LPS may alter HAS stability on the plasma membrane. However, no statistically significant changes in EV shedding were detected, as observed before in macrophages [40].

Hyaluronan content of the EVs reflect the HA synthesis activity of parental cells

A high concentration of HA (11 ng/10,000 cells/24 h) was detected in the EV fractions isolated from the hMSCs, which indicates that considerable amounts of HA can be carried on the surface of the vesicles. However, it is surprising that the relative proportion of total HA secreted by the hMSCs (2.9%) was rather low in the EV fraction, even though a high number of HA-positive EVs were detected in the live cell cultures. We hypothesize that the shearing forces during centrifugation steps may have resulted in partial shedding of the HA coat from the surface of the EVs.

It has been shown that HAS activity is associated with shedding of the EVs in many cell types [23,28,42]. However, the inhibition of HAS2 and HAS3 expression did not affect the EV shedding activity of the hMSCs in the present study. 4-methylumbelliferone (4-MU) [43] inhibits HA synthesis [46] by several mechanisms, such as depleting the intracellular UDP-glucuronic acid pool and reducing HAS2 and HAS3 mRNA levels [44,45]. Interestingly, EMT is blocked by inhibiting HA synthesis with 4-MU in canine mammary tumor cells [46], and 4-MU has been shown to suppress LPS-induced inflammation [39]. As expected, 4-MU inhibited expression levels of HASes, HA secretion, and the formation of HA-coated filopodia. However, the number of secreted particles was not affected by 4-MU, which is not in line with recent work showing that 4-MU inhibited HAS3-positive EV shedding in HAS3-overexpressing MV3 cells [42]. Interestingly, while 4-MU significantly inhibited HAS1 and HAS2 levels, the HAS3 levels increased, which may explain the rather small effect on HA secretion levels and lack of effect on EV shedding.

Overall, the results of this work suggest that small fluctuations in HA synthesis activity do not affect the EV secretion of stem cells. However, the obtained results demonstrate that the HA content of the released EVs reflects the changes in HA synthesis activity of the parental cells, which may have an impact on the biological properties of the EVs, and could be utilized in diagnostics and disease monitoring.

HA-coated EVs are potential mediators of the MSC-mediated functions in tissue healing and regeneration

The main finding of this work is that the EVs secreted by the hMSCs carry HA on their surface. This is of great importance because interactions between stem cells and the microenvironment have been suggested to play a critical role in determining stem cell phenotype. Hyaluronan interacts with various matrix components, such as proteins and proteoglycans to organize the ECM and to maintain tissue homeostasis. It also mediates the functions of stem cells [47] in healing and protection processes [48] by creating a niche that regulates stem cell differentiation and survival [15].

The MSCs have raised major interest in regenerative medicine because of their differentiation capacity into various cell types. The MSCs used in this study have been previously shown to have potential to differentiate into chondrocytes, osteoblasts, and adipocytes [49]. Increasing evidence indicates that EVs are one of the major components mediating the therapeutic efficacy of MSCs [1,3]. Many recent studies suggest that the EVs originating from the MSCs mediate the healing of injuries such as acute kidney injury [29], myocardial ischemia [50], and chronic heart failure [51]. The EVs and HA carried on them are important components of the microenvironment that support stem cells and help to replace damaged ECM in injured tissues. Furthermore, HA-carrying EVs potentially induce local effects in the extracellular space adjacent to the cell of origin, but may also mediate systemic effects if released to the circulation.

Conclusions

This study shows that the EVs secreted by the hMSCs act as carriers for HA on their surfaces, and are potential paracrine mediators of the MSCs. The HA-EVs and signals within them may participate in the ECM remodeling directly or indirectly by interacting with ECM-producing cells. Furthermore, HA coating may the reduce immunogenicity of the EVs and facilitate their binding to target cells via CD44 interactions. The results of this study support the hypothesis that the secretion of HA-carrying EVs is a general process. Therefore, in the future it is important to clarify the factors that regulate their excretion, and to find novel methods for their identification as well as for studying their functional effects on target cells.

Supplementary data to this article can be found online at http://dx.doi.org/10.1016/j.matbio.2017.05.001.

Acknowledgements

Financial support for this study was provided by the Academy of Finland (grants #276426 & #284520), Otto Malm Foundation, K. Albin Johanssons Stiftelse Foundation, Kuopio University Foundation, and Northern Savo Cancer Foundation. The authors want to thank Virpi Miettinen for technical assistance. We are thankful for the opportunity to use the facilities of the SIB Labs.

Received 30 March 2017;
Received in revised form 27 April 2017;
Accepted 2 May 2017
Available online 5 May 2017

Keywords:
Hyaluronan;
CD44;
Extracellular vesicle;
Stem cell;
Filopodia;
Hyaluronan synthase

Abbreviations used:
4-MU, 4-methylumbelliferone; BSA, bovine serum albumin; CD44, hyaluronan receptor, cluster of

differentiation 44; CLEM, correlative light and electron microscopy; GFP, green fluorescent protein; ECM, extracellular matrix; EM, electron microscope; EV, extracellular vesicle; HA, hyaluronan; HABC, hyaluronan binding complex of the cartilage aggrecan G1; HAS, hyaluronan synthase; HBSS, Hank's balanced salt solution; LPS, lipopolysaccharide; MSC, mesenchymal stem cell; NTA, nanoparticle tracking analysis; PBS, phosphate-buffered saline.

References

[1] M. Motavaf, K. Pakravan, S. Babashah, F. Malekvandfard, M. Masoumi, M. Sadeghizadeh, Therapeutic application of mesenchymal stem cell-derived exosomes: a promising cell-free therapeutic strategy in regenerative medicine, Cell. Mol. Biol. (Noisy-le-grand) 62 (2016) 74–79.

[2] D.G. Phinney, M.F. Pittenger, Concise review: MSC-derived exosomes for cell-free therapy, Stem Cells 35 (2017) 851–858.

[3] A. Marote, F.G. Teixeira, B. Mendes-Pinheiro, A.J. Salgado, MSCs-derived exosomes: cell-secreted Nanovesicles with regenerative potential, Front. Pharmacol. 7 (2016) 231.

[4] A.J. Friedenstein, I.I. Piatetzky-Shapiro, K.V. Petrakova, Osteogenesis in transplants of bone marrow cells, J. Embryol. Exp. Morpholog. 16 (1966) 381–390.

[5] H.S. Kim, D.Y. Choi, S.J. Yun, S.M. Choi, J.W. Kang, J.W. Jung, D. Hwang, K.P. Kim, D.W. Kim, Proteomic analysis of microvesicles derived from human mesenchymal stem cells, J. Proteome Res. 11 (2012) 839–849.

[6] S. Rani, A.E. Ryan, M.D. Griffin, T. Ritter, Mesenchymal stem cell-derived extracellular vesicles: toward cell-free therapeutic applications, Mol. Ther. 23 (2015) 812–823.

[7] G. Camussi, M.C. Deregibus, S. Bruno, V. Cantaluppi, L. Biancone, Exosomes/microvesicles as a mechanism of cell-to-cell communication, Kidney Int. 78 (2010) 838–848.

[8] N. Javeed, D. Mukhopadhyay, Exosomes and their role in the micro-/macro-environment: a comprehensive review, J. Biomed. Res. 30 (2016)http://dx.doi.org/10.7555/JBR.30.20150162.

[9] L. Huleihel, G.S. Hussey, J.D. Naranjo, L. Zhang, J.L. Dziki, N.J. Turner, D.B. Stolz, S.F. Badylak, Matrix-bound nanovesicles within ECM bioscaffolds, Sci. Adv. 2 (2016), e1600502.

[10] F. Fatima, M. Nawaz, Stem cell-derived exosomes: roles in stromal remodeling, tumor progression, and cancer immunotherapy, Chin. J. Cancer 34 (2015) 541–553.

[11] F. Collino, M.C. Deregibus, S. Bruno, L. Sterpone, G. Aghemo, L. Viltono, C. Tetta, G. Camussi, Microvesicles derived from adult human bone marrow and tissue specific mesenchymal stem cells shuttle selected pattern of miRNAs, PLoS One 5 (2010), e11803.

[12] L.A. Reis, F.T. Borges, M.J. Simoes, A.A. Borges, R. Sinigaglia-Coimbra, N. Schor, Bone marrow-derived mesenchymal stem cells repaired but did not prevent gentamicin-induced acute kidney injury through paracrine effects in rats, PLoS One 7 (2012), e44092.

[13] P.H. Weigel, V.C. Hascall, M. Tammi, Hyaluronan synthases, J. Biol. Chem. 272 (1997) 13997–14000.

[14] T. Chanmee, P. Ontong, N. Itano, Hyaluronan: a modulator of the tumor microenvironment, Cancer Lett. 375 (2016) 20–30.

[15] D.N. Haylock, S.K. Nilsson, The role of hyaluronic acid in hemopoietic stem cell biology, Regen. Med. 1 (2006) 437–445.

[16] V.J. Coulson-Thomas, T.F. Gesteira, V. Hascall, W. Kao, Umbilical cord mesenchymal stem cells suppress host rejection: the role of the glycocalyx, J. Biol. Chem. 289 (2014) 23465–23481.

[17] M.F. Pittenger, A.M. Mackay, S.C. Beck, R.K. Jaiswal, R. Douglas, J.D. Mosca, M.A. Moorman, D.W. Simonetti, S. Craig, D.R. Marshak, Multilineage potential of adult human mesenchymal stem cells, Science 284 (1999) 143–147.

[18] I. Morath, T.N. Hartmann, V. Orian-Rousseau, CD44: more than a mere stem cell marker, Int. J. Biochem. Cell Biol. 81 (2016) 166–173.

[19] P.Y. Chen, L.L. Huang, H.J. Hsieh, Hyaluronan preserves the proliferation and differentiation potentials of long-term cultured murine adipose-derived stromal cells, Biochem. Biophys. Res. Commun. 360 (2007) 1–6.

[20] A.K. Jha, X. Xu, R.L. Duncan, X. Jia, Controlling the adhesion and differentiation of mesenchymal stem cells using hyaluronic acid-based, doubly crosslinked networks, Biomaterials 32 (2011) 2466–2478.

[21] C. Qu, K. Rilla, R. Tammi, M. Tammi, H. Kröger, M.J. Lammi, Extensive CD44-dependent hyaluronan coats on human bone marrow-derived mesenchymal stem cells produced by hyaluronan synthases HAS1, HAS2 and HAS3, Int. J. Biochem. Cell Biol. 48 (2014) 45–54.

[22] A. Kultti, K. Rilla, R. Tiihonen, A.P. Spicer, R.H. Tammi, M.I. Tammi, Hyaluronan synthesis induces microvillus-like cell surface protrusions, J. Biol. Chem. 281 (2006) 15821–15828.

[23] K. Rilla, S. Pasonen-Seppänen, A.J. Deen, V.V. Koistinen, S. Wojciechowski, S. Oikari, R. Kärnä, G. Bart, K. Törrönen, R.H. Tammi, M.I. Tammi, Hyaluronan production enhances shedding of plasma membrane-derived microvesicles, Exp. Cell Res. 319 (2013) 2006–2018.

[24] G.V. Shelke, C. Lasser, Y.S. Gho, J. Lotvall, Importance of exosome depletion protocols to eliminate functional and RNA-containing extracellular vesicles from fetal bovine serum, J. Extracell Vesicles 3 (2014)http://dx.doi.org/10.3402/jev.v3.24783 (eCollection 2014).

[25] K. Rilla, R. Tiihonen, A. Kultti, M. Tammi, R. Tammi, Pericellular hyaluronan coat visualized in live cells with a fluorescent probe is scaffolded by plasma membrane protrusions, J. Histochem. Cytochem. 56 (2008) 901–910.

[26] K. Rilla, A. Koistinen, Correlative light and electron microscopy reveals the HAS3-induced dorsal plasma membrane ruffles, Int. J. Cell. Biol. 2015 (2015) 769163.

[27] E.L. Hiltunen, M. Anttila, A. Kultti, K. Ropponen, J. Penttinen, M. Yliskoski, A.T. Kuronen, M. Juhola, R. Tammi, M. Tammi, V.M. Kosma, Elevated hyaluronan concentration without hyaluronidase activation in malignant epithelial ovarian tumors, Cancer Res. 62 (2002) 6410–6413.

[28] K. Rilla, H. Siiskonen, M. Tammi, R. Tammi, Hyaluronan-coated extracellular vesicles-a novel link between hyaluronan and cancer, Adv. Cancer Res. 123 (2014) 121–148.

[29] S. Bruno, C. Grange, M.C. Deregibus, R.A. Calogero, S. Saviozzi, F. Collino, L. Morando, A. Busca, M. Falda, B. Bussolati, C. Tetta, G. Camussi, Mesenchymal stem cell-derived microvesicles protect against acute tubular injury, J. Am. Soc. Nephrol. 20 (2009) 1053–1067.

[30] M. Morello, V.R. Minciacchi, P. de Candia, J. Yang, E. Posadas, H. Kim, D. Griffiths, N. Bhowmick, L.W. Chung, P. Gandellini, M.R. Freeman, F. Demichelis, D. Di Vizio, Large oncosomes mediate intercellular transfer of functional microRNA, Cell Cycle 12 (2013) 3526–3536.

[31] S.M. Johnson, C. Dempsey, C. Parker, A. Mironov, H. Bradley, V. Saha, Acute lymphoblastic leukaemia cells

produce large extracellular vesicles containing organelles and an active cytoskeleton, J. Extracell Vesicles 6 (2017) 1294339.
[32] T. Ramos, L. Sanchez-Abarca, S. Muntion, S. Preciado, N. Puig, G. Lopez-Ruano, A. Hernandez-Hernandez, A. Redondo, R. Ortega, C. Rodriguez, F. Sanchez-Guijo, C. Del Canizo, MSC surface markers (CD44, CD73, and CD90) can identify human MSC-derived extracellular vesicles by conventional flow cytometry, Cell Commun. Signal 14 (2016) 2.
[33] V. Koistinen, K. Härkönen, R. Kärnä, U.T. Arasu, S. Oikari, K. Rilla, EMT induced by EGF and wounding activates hyaluronan synthesis machinery and EV shedding in rat primary mesothelial cells, Matrix Biol. (2016) http://dx.doi.org/10.1016/j.matbio.2016.12.007.
[34] E. Karousou, S. Misra, S. Ghatak, K. Dobra, M. Gotte, D. Vigetti, A. Passi, N.K. Karamanos, S.S. Skandalis, Roles and targeting of the HAS/hyaluronan/CD44 molecular system in cancer, Matrix Biol. (2016) http://dx.doi.org/10.1016/j.matbio.2016.10.001.
[35] M. Zoller, CD44, Hyaluronan, the Hematopoietic Stem Cell, and Leukemia-Initiating Cells, Front. Immunol. 6 (2015) 235.
[36] W. Mu, S. Rana, M. Zöller, Host matrix modulation by tumor exosomes promotes motility and invasiveness, Neoplasia 15 (2013) 875–887.
[37] R.H. Tammi, A.G. Passi, K. Rilla, E. Karousou, D. Vigetti, K. Makkonen, M.I. Tammi, Transcriptional and post-translational regulation of hyaluronan synthesis, FEBS J. 278 (2011) 1419–1428.
[38] F. Li, P. Hao, G. Liu, W. Wang, R. Han, Z. Jiang, X. Li, Effects of 4-methylumbelliferone and high molecular weight hyaluronic acid on the inflammation of corneal stromal cells induced by LPS, Graefes Arch. Clin. Exp. Ophthalmol. (2016).
[39] R.J. McKallip, H. Ban, O.N. Uchakina, Treatment with the hyaluronic Acid synthesis inhibitor 4-methylumbelliferone suppresses LPS-induced lung inflammation, Inflammation 38 (2015) 1250–1259.
[40] M.Y. Chang, Y. Tanino, V. Vidova, M.G. Kinsella, C.K. Chan, P.Y. Johnson, T.N. Wight, C.W. Frevert, Reprint of: a rapid increase in macrophage-derived versican and hyaluronan in infectious lung disease, Matrix Biol. 35 (2014) 162–173.
[41] D. Ti, H. Hao, C. Tong, J. Liu, L. Dong, J. Zheng, Y. Zhao, H. Liu, X. Fu, W. Han, LPS-preconditioned mesenchymal stromal cells modify macrophage polarization for resolution of chronic inflammation via exosome-shuttled let-7b, J. Transl. Med. 13 (2015) 308 (015-0642-6).
[42] A.J. Deen, U.T. Arasu, S. Pasonen-Seppänen, A. Hassinen, P. Takabe, S. Wojciechowski, R. Kärnä, K. Rilla, S. Kellokumpu, R. Tammi, M. Tammi, S. Oikari, UDP-sugar substrates of HAS3 regulate its O-GlcNAcylation, intracellular traffic, extracellular shedding and correlate with melanoma progression, Cell. Mol. Life Sci. 73 (2016) 3183–3204.
[43] T. Nakamura, K. Takagaki, S. Shibata, K. Tanaka, T. Higuchi, M. Endo, Hyaluronic-acid-deficient extracellular matrix induced by addition of 4-methylumbelliferone to the medium of cultured human skin fibroblasts, Biochem. Biophys. Res. Commun. 208 (1995) 470–475.
[44] I. Kakizaki, K. Kojima, K. Takagaki, M. Endo, R. Kannagi, M. Ito, Y. Maruo, H. Sato, T. Yasuda, S. Mita, K. Kimata, N. Itano, A novel mechanism for the inhibition of hyaluronan biosynthesis by 4-methylumbelliferone, J. Biol. Chem. 279 (2004) 33281–33289.
[45] A. Kultti, S. Pasonen-Seppänen, M. Jauhiainen, K.J. Rilla, R. Kärnä, E. Pyoriä, R.H. Tammi, M.I. Tammi, 4-Methylumbelliferone inhibits hyaluronan synthesis by depletion of cellular UDP-glucuronic acid and downregulation of hyaluronan synthase 2 and 3, Exp. Cell Res. 315 (2009) 1914–1923.
[46] T. Saito, T. Dai, R. Asano, The hyaluronan synthesis inhibitor 4-methylumbelliferone exhibits antitumor effects against mesenchymal-like canine mammary tumor cells, Oncol. Lett. 5 (2013) 1068–1074.
[47] M.A. Solis, Y.H. Chen, T.Y. Wong, V.Z. Bittencourt, Y.C. Lin, L.L. Huang, Hyaluronan regulates cell behavior: a potential niche matrix for stem cells, Biochem. Res. Int. 2012 (2012) 346972.
[48] D. Jiang, J. Liang, P.W. Noble, Hyaluronan in tissue injury and repair, Annu. Rev. Cell Dev. Biol. 23 (2007) 435–461.
[49] C. Qu, S. Kaitainen, H. Kröger, R. Lappalainen, M.J. Lammi, Behavior of human bone marrow-derived mesenchymal stem cells on various titanium-based coatings, 9 (10) (2016) 827.
[50] R.C. Lai, F. Arslan, M.M. Lee, N.S. Sze, A. Choo, T.S. Chen, M. Salto-Tellez, L. Timmers, C.N. Lee, R.M. El Oakley, G. Pasterkamp, D.P. de Kleijn, S.K. Lim, Exosome secreted by MSC reduces myocardial ischemia/reperfusion injury, Stem Cell Res. 4 (2010) 214–222.
[51] A. Kervadec, V. Bellamy, N. El Harane, L. Arakelian, V. Vanneaux, I. Cacciapuoti, H. Nemetalla, M.C. Perier, H.D. Toeg, A. Richart, M. Lemitre, M. Yin, X. Loyer, J. Larghero, A. Hagege, M. Ruel, C.M. Boulanger, J.S. Silvestre, P. Menasche, N.K. Renault, Cardiovascular progenitor-derived extracellular vesicles recapitulate the beneficial effects of their parent cells in the treatment of chronic heart failure, J. Heart Lung Transplant. 35 (2016) 795–807.